Semantic-based Biomedical Image Indexing and Retrieval

Y. Liu[a], N. A. Lazar[b], W. E. Rothfus[c], F. Dellaert[d],
A. Moore[a], J. Schneider[a] and T. Kanade[a]

[a] The Robotics Institute
[b] Statistics Department
Carnegie Mellon University, 5000 Forbes Ave.,
Pittsburgh, PA 15213, USA
[c] University of Pittsburgh Medical Center, Pittsburgh, PA, USA
[d] Georgia Institute of Technology, Atlanta, Georgia 30332 USA
Contact: yanxi@cs.cmu.edu, 412-268-6234

December 30, 2003

ABSTRACT

This paper summarizes our work and our understanding on volumetric pathological neuroimage retrieval under the framework of classification-driven feature selection. The main effort concerns off-line image feature space reduction for improved image indexing feature discriminating power as well as reduced computational cost during on-line pathological neuroimage retrieval.
Keywrods: 3D image, feature selection, brain asymmetry, midsagittal plane, image classification,indexing, retrieval

1 Motivation

As the national and private sectors commit more and more of their data resources to electronic form, on-line image data is expanding rapidly in quantity, content and dimension. The utilization of such large data sets for research and education, on the other hand, is quite limited due to the lack of intelligent, effective image indexing and retrieval capabilities. Given the current trend towards "paper-less" hospitals, the commercially available Picture Archiving and Communication System (PACS) installed in many hospitals across the world collects several terabytes of on-line image data in individual hospitals monthly, weekly, even daily [8]. The access to such data is usually restricted by using patient names and patients' identification numbers [26]. There exists a large demand for computer technology that goes beyond data storage to retrieve images by *image content* [8, 20, 26]. A distinction between two types of "contents" of an image should be made: one refers to the make-up of an image, for example, color, texture, local or global compositions etc., and the other refers to the meaning of an image, for example, an apple, a horse or a brain tumor of type X at anatomic location Y. The first type of image content is the *image syntax* content and the second type *image semantics*.

Biomedical images form an essential and inseparable component of diagnosis, intervention and patient follow-ups. It is therefore natural to use these images as a front-end index to retrieve medically relevant cases from digital patient databases. Existing "content-based" image retrieval (CBIR) systems for general-purpose image databases, e.g. [5, 17, 16, 18, 24], use visual features such as color and texture (e.g. color/intensity histogram, color layout and region-based methods) for image retrieval on large, diverse, two-dimensional (2D) general purpose image sets with good performance. Usually, the global statistical color and texture measures do not necessarily reflect or have a proven correspondence to its *image semantics*.

Using text for medical database indexing and retrieval has been traditionally the dominant approach for semantics based image database access (e.g. [1]). Text-based methods are based on different predefined key words and category hierarchies. There are some existing, albeit controversial, labeling codes for disease classification, such as Unified Medical Language System (UMLS) and International Classification of Diseases 9th Revision (ICD9). On the other hand, annotation of images using such coding systems becomes unpractical with the rapid increase of the amount of image data; and these coding systems are limited by their predefined vocabularies, which could be subjective, incomplete, coarse, and ambiguous [20]. Image data provides a complementary source of information that is an objective and precise description of the disease state.

Biomedical images differ from general purpose images in many ways: First of all, color is often not the main characteristic in a biomedical image, especially CT and MR images. Secondly, sample differences are usually very small. Sometimes these types of domain-specific differences are subtle to an untrained eye. Many well-studied image features (e.g. color) for general purpose image indexing may fail to be effective discriminators for image sets taken within a single biomedical domain. Thirdly, a majority of biomedical images captures human anatomy that is in nature a three dimensional structure. For an example, see Figure 1. Therefore,

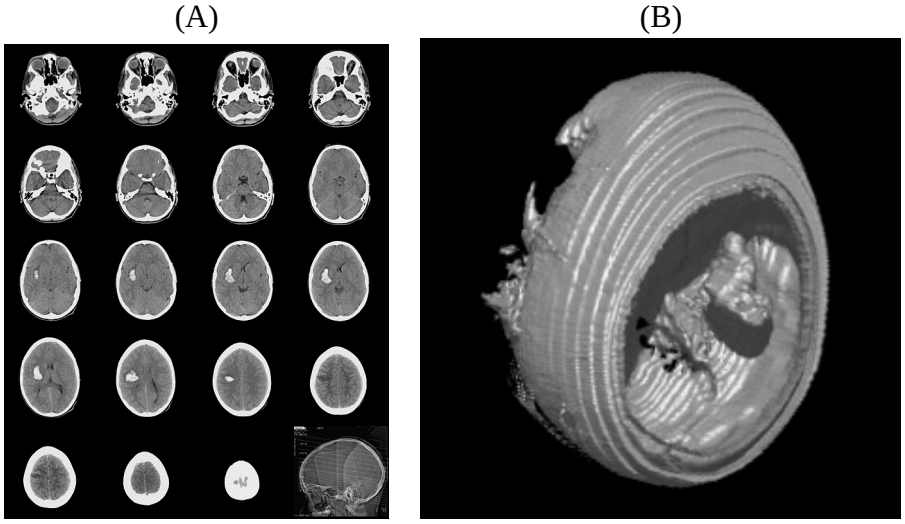

Figure 1: (A): A sample volumetric image is shown, composed of a set of parallel clinical CT scans (axial). This is a case of acute right basal ganglion bleed. (B): A 3D visualization of the CT scan (left) shows the appearance of the lesion with respect to the skull.

image registration becomes necessary before volumetric image comparisons and image feature extraction. Finally, a major difference between biomedical and general purpose image retrieval is the stability of image semantic contents. Medical images from a particular medical domain usually provide objective, semantically well-defined image classes while the semantics of the general purpose images can be subjectively determined and vary from time to time, person to person, and domain to domain.

This last difference between the two image sets presents difficulties in off-line learning of semantically relevant image features for general purpose CBIR; alternatively, this learning process is often accomplished on-line with user feedback

[14, 2]. Given image class stability and objectiveness for large biomedical image set, it is feasible to learn class discriminative biomedical image features off-line.

The focus of this chapter is to demonstrate, using a clinical neuroimage dataset example, how to learn image features that reflect image semantics off-line for on-line image retrieval. A basic framework for classification-driven semantic based image retrieval is shown in Figure 2, containing two stages with five essential components. The two stages are an off-line stage for classification-driven image similarity metric learning (feature weighting), and an on-line stage for image retrieval. The five essential components are (1) image preprocessing, (2) image feature extraction, (3) feature subset weighting via image classification, (4) image retrieval, and (5) quantitative evaluation. Though the two stages share some common components, the goals and constraints differ. In the off-line stage the goal is to find the best and smallest subset of image features that capture image semantics. It requires an explicitly labeled image data set and sufficient computer memory space to store a large feature attribute matrix and to support extensive search on this matrix. High computational speed is a plus but not necessary. During the on-line stage, on the other hand, the demands are fast retrieval speed and visualization of retrieved images given a similarity metric and a query image.

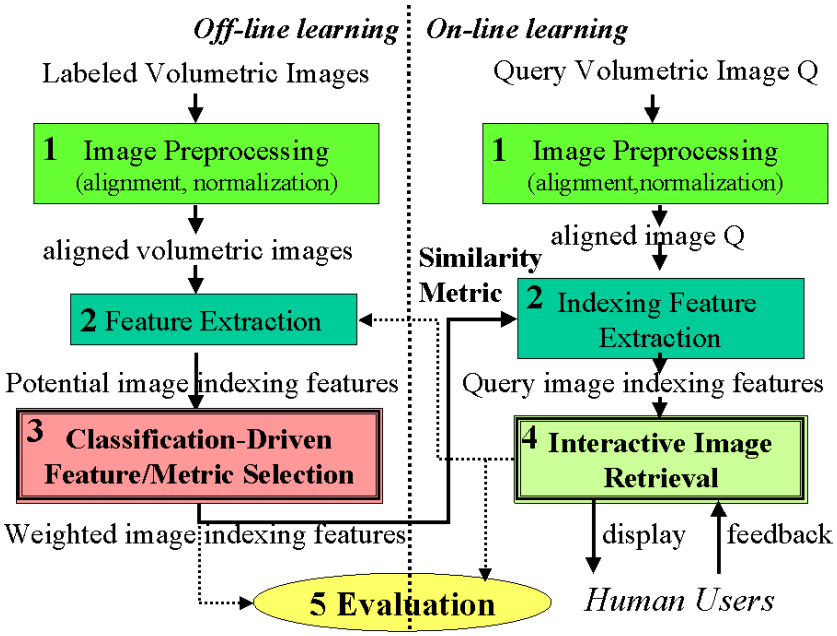

Figure 2: Basic components for classification-driven semantic image retrieval

2 Approach

Using a neuroimage database composed of clinical volumetric CT image sets of hemorrhage (blood), bland infarct (stroke) and normal brains, we have explored various issues in medical image analysis, indexing and retrieval [10, 9, 11]. The image semantics in this context is expressed as the image pathology. For example, *normal*, *right basal ganglion acute bleed* or *frontal lobe acute infarct*. Figure 3

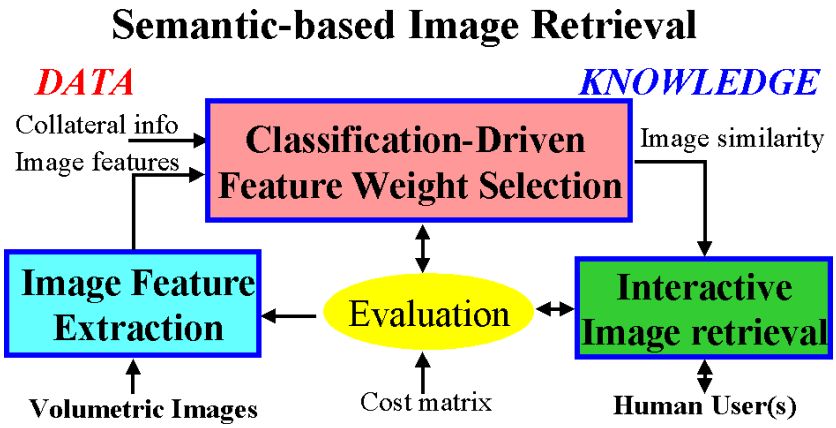

Figure 3: Overview of a semantic-based classification-driven image retrieval framework.

shows three major components in an image retrieval system. The focus of this chapter is on the second component: feature subspace reduction for increased discriminating power in a learned similarity metric. The three major components in this framework are

- (1) **Feature extraction** maps each volumetric image into a multi-dimensional image feature space;
- (2) **Feature selection** determines the dimension and relative weighting of a discriminative feature subspace and selects a similarity metric for image indexing and comparison; and
- (3) **Adaptive image retrieval** captures user intentions by tuning to the most suitable image similarity measure.

For each given image database **B** and a set of potential image features F_B extracted from each image in the database, we define two basic parameters:

1. the **fundamental dimension** of the database is the lowest feature subspace dimension such that the discriminative power of the subspace is no less than the original feature space;

2. the semantic class **separability** within the database is a quantitative measure for how well image classes are separated.

Our research goal is to construct a systematic framework to learn these two parameters through classification-driven semantic-based image feature space reduction. The net result of the feature space reduction in image retrieval application includes: (1) reduced computational cost during image retrieval; (2) effective scalability to larger image datasets; and (3) improved discriminating power for finding similar images at retrieval time.

More formally, given an image database **B** and a set of potential indexing features $F_B = \{f_1, f_2, ..., f_n\}$ which we call the original feature space of dimension n, *feature space reduction* is defined as a mapping from F_B to a weighted feature space $F_W = \{w_1 f_1, w_2 f_2, ..., w_n f_n\}$ where $0 \leq w_i \leq 1$. Since some of the w_is may equal 0, $|F_W| \leq |F_B|$. If d is the number of non-zero weights w_i above a certain threshold ϵ, the ratio n/d is called the *reduction ratio*. The number d is an indication of the fundamental dimension of the database under F_B. The classification rate (using k-NN classifier for example) under the chosen fundamental dimension of the image set would be a good indicator of the class separability. Two types of features are expected to be removed from F_B during feature space reduction: irrelevant features and redundant features. As a result, for any image semantic class c_i the posterior probabilities $P(c_i|F_B)$ and $P(c_i|F_W)$ are equivalent since class irrelevant and redundant features are excluded from F_W.

3 Classification-Driven Feature Space Reduction

We use a novel midsagittal plane method for 3D pathological neuroimage alignment [9]. Global and local statistical image features are extracted for describing brain asymmetry [11], geometry and texture properties. These features form the initial, high-dimensional feature space. There are many existing feature space reduction approaches, not all of which are appropriate for image retrieval. We are looking for methods that can truly reduce computational cost by explicitly weighting each existing feature dimension (so that we can discard unnecessary feature dimensions during on-line retrieval). Principal component analysis, for instance, though it gives an estimate of the fundamental dimensions for data representations

Feature Space Reduction Method	Reduced Feature SpaceDimension (fold)	CR Improved
MemoryBasedLearning (holdout)	5 - 10 (5-10)	15%
ClassificationTree (holdout)	2-4 (12-24)	8%
ClassificationTree (LOO)	3-5 (9-15)	5%
Discriminant Analysis (holdout)	6-10 (5-7)	19%
Discriminant Analysis (LOO)	12-15 (3-4)	29%

Table 1: The original feature space dimension is 46. This table shows the feature space dimension reduction rates after feature selection, in actual dimensions and in fold. Also shown is the classification rate (CR) improvement over the original feature space. Here *holdout* means separating the original dataset into a training set (2/3 data) and a *holdout* test set (1/3 data), training the classifier on the training set and evaluating results using the test set. LOO = *Leave One Out* strategy, it uses each data point as a test set once and the rest of the data points as a training set in turn.

not for data discrimination, does not meet this standard. Artificial neural networks do not provide the explicit weightings desired for image retrieval either.

Table 1 records the results from feature space reduction using three very different methods: memory-based learning, classification trees and discriminant analysis. All the experiments are carried out on an image dataset containing 48 3D brains with three broad pathology classes: normal (26), blood (8) and stroke (14). The initial feature space is 46 dimensions composed of statistical measurements describing human brain asymmetry [11, 9].

Memory Based Learning In [11] we have reported in detail our initial effort on finding the most discriminating feature subset(s) using a memory-based learning approach, Bayes classifier, Parzen windows and a non-deterministic search engine. The average precision rate for image retrieval across different pathologies is about 80%.

Classification Trees A binary classification tree is constructed by finding the best binary split among the features at each step [23]. Based on a multinomial probability model, we define a *deviance* for the tree: $D = \sum_i D_i$ where $D_i = -2 \sum_k n_{ik} \log p_{ik}$ as a sum over leaves. The 'best' split is the maximum reduction in *deviance* over all leaves. The tree grows until each leaf is homogeneous enough (its deviance is less than certain value). We randomly divided the dataset 50 times into 2/3-1/3 training-testing pairs. A tree was grown on each of

the 50 training sets. Results are listed in Table 1.

Discriminant Analysis A combination of forward selection [23] and linear discriminant analysis is used with two different criteria for selecting features: (1) the augmented variance ratio, which compares within-group and between-group variances and penalizes features where class means are too close together, and (2) Wilks' lambda, which measures dissimilarity among groups. Results on feature space reduction over 50 randomly divided training-testing pairs are shown in Table 1.

4 Experiments

A feasibility study for image retrieval was performed using a data set of 48 volumetric CT brain scans containing normal (26), stroke (14) and blood cases (8). These are clinical CT images collected directly from a local hospital emergency room. Three image semantic classes are used: normal brains, stroke (without bleeding) brains and brains with blood (Figure 4). A sample of input brain scans (shown in 2D slices) is displayed in Figure 5.

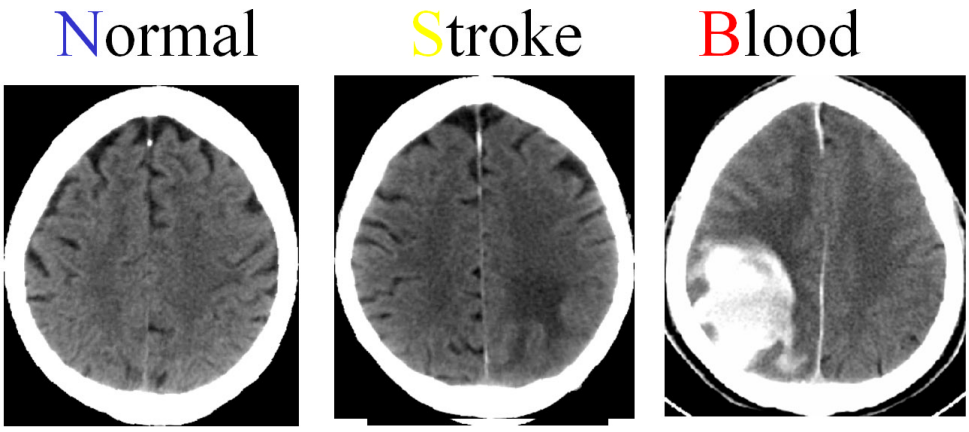

Figure 4: The approximate corresponding slices (before registration) of three brains, each from one of the three semantic classes: normal, stroke and blood.

4.1 Image Alignment

We define an *ideal head coordinate system* centered in the brain with positive X_0, Y_0 and Z_0 axes pointing in the right, anterior and superior directions respec-

Examples of pathological brain images

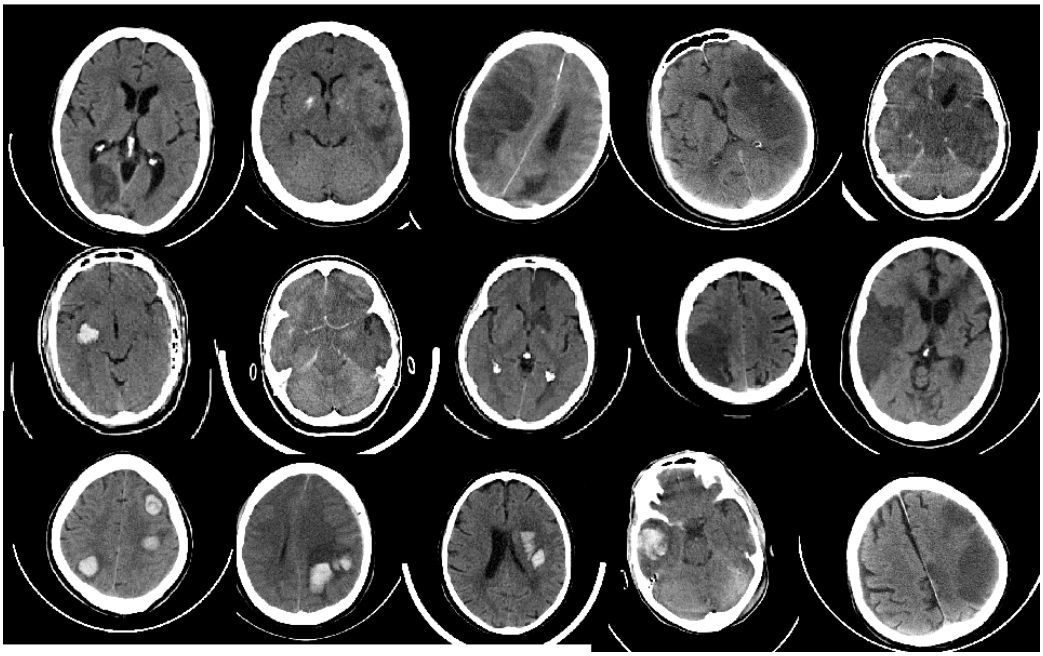

Figure 5: Several sample pathological brain images

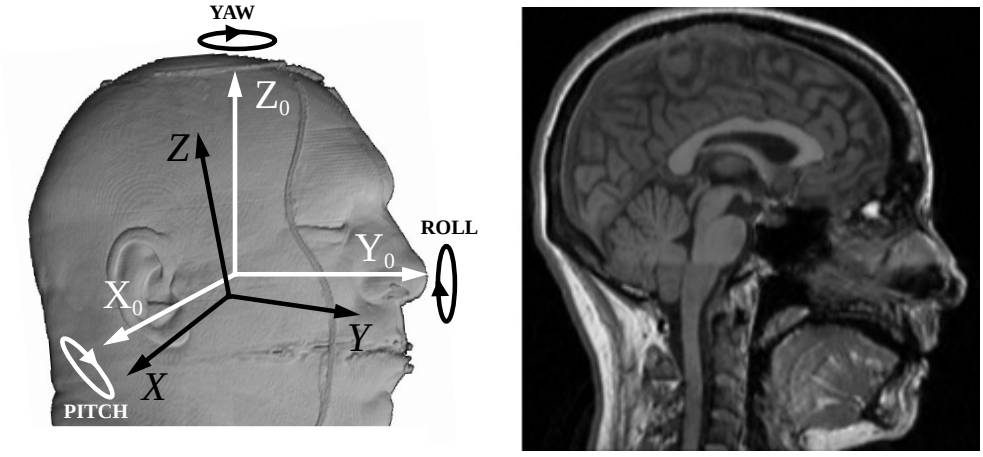

(a) $X_0Y_0Z_0$ v. XYZ (b) $X_0 = 0$

Figure 6: (a) Ideal head coordinate system $X_0Y_0Z_0$ vs. the working coordinate system XYZ. X and Y are oriented along the rows and columns of each image slice, and Z is the actual axis of the scan. Rendered head courtesy of the Visible Human Project. (b) The midsagittal plane automatically extracted using our MSP extraction algorithm.

tively (Figure 6, white coordinate axes) consistent with the Talairach framework [21]. With respect to this coordinate system, the MSP of the brain is defined as the plane $X_0 = 0$. The effect of the ideal midsagittal plane (iMSP) extraction algorithm [9] is to find where the MSP is supposed to be, especially, for pathology brains where the anatomic midsagittal plane is often distorted (shifted or bent) due to large lesions. Figure 7 shows some 2D sample results after the midsagittal plane is extracted. The iMSP algorithm is robust under adverse conditions and has been evaluated extensively [9]. Axial and coronal slices are used simultaneously to handle large out-of-plane rotation angles effectively. No statistically significant difference is found between the iMSP algorithm and two experienced neuroradiologists. The first step is to align all 3D images such that the ideal midsagittal planes (iMSP) of different brain images are parallel and pitch angle is zero. 3D image intra- and inter-subject, multi-modality rigid and deformable registrations of normal brains have achieved excellent results [25, 13]. However, no existing technology is readily available for registration of single or multi-modality, inter-subject, pathological brain images [7]. Matching two 3D pathological brains remains a difficult and controversial problem. This situation poses challenges to any

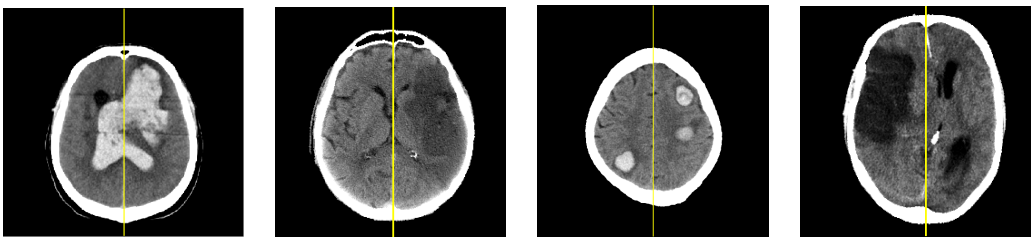

Figure 7: The ideal symmetry axis is extracted as the intersection of a 3D brain image (CT) and its ideal midsagittal plane.

3D pathological neuroimage databases, especially for CT images. In our work, we have taken advantage of the approximate bilateral structure of human brains to develop a robust midsagittal plane (MSP) extraction algorithm [9] for pathological brain alignment and comparison.

4.2 Potential Indexing Feature Extraction

Though lesions are usually obvious to a trained eye, automatic image segmentation is a very hard problem in medical image analysis [4]. We take an alternative approach for image feature extraction that does not require precise segmentation of the image: human brains present an approximate bilateral symmetry, from which pathological brains often depart. Even the brains where pathology appears symmetrically present a different kind of symmetry from normal brains. Our intention is to quantify and capture the statistical distribution difference of various brain asymmetries. A set of relatively simple and computationally inexpensive statistical image features is collected (Figure 8). After the iMSP is aligned in the middle of each 3D volumetric image (leftmost image in Figure 8), three types of asymmetry features are computed: 1) global statistical properties, 2) measures of asymmetry of halved and quartered brains, and 3) local asymmetrical region-based properties. These features are extracted from the original image (Fig. 8, image I) with its iMSP aligned, the difference image (Fig. 8, image D) of the original image and its mirror reflection with respect to iMSP, the thresholded difference image (image G[1]), and the original image masked by the thresholded binary image (Figure 8, image M). The image features include: the means, the

[1]In our implementation, the absolute value of image G is used; this value quantifies how asymmetrical the corresponding voxel regions are.

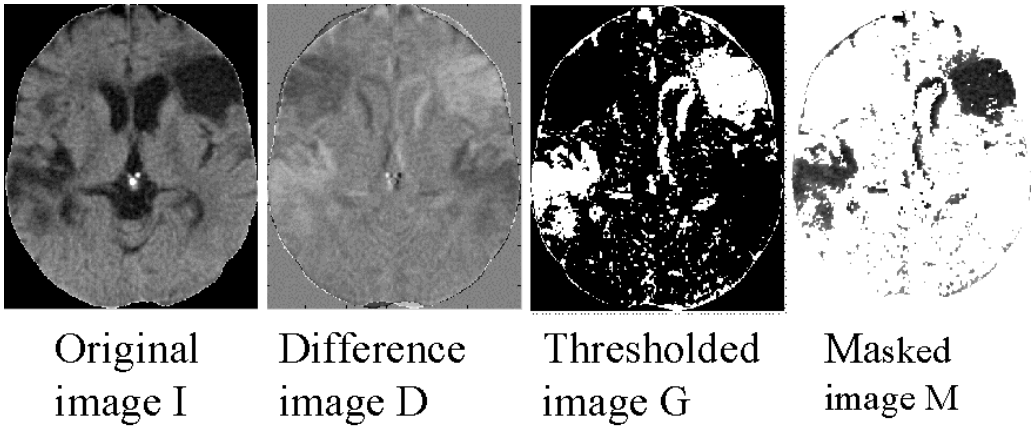

Figure 8: **Image I**: original image with its 3D MSP aligned and centered vertically. **Image D**: the intensity difference image between the original image I and its own vertical reflection. **Image G**: a thresholded image of image D. **Image M**: the product of image G with original image I (a masked image).

variances, and the X and Y gradients of the intensity images at different regions and under various Gaussian smoothing, scaling and thresholding. A total of 48 image features are computed from each image.

4.3 Classification-Driven Feature Subset Evaluation

Now each image i becomes a vector V_i, and the length $N = |V_i|$ is the total dimension of the potential image feature space computed above. All the image data in the database form an $M \times N$ 2D sheet with M image points in the N dimensional feature space. A labeling, given by an experienced neuroradiologist, is added to the end of each row indicating the semantic class of the image, either simply the pathology type or pathology plus the anatomical location of the lesion(s).

We use a CMU proprietary combinatorial search engine called "Vizier" [19], to simultaneously find the image feature sub-dimensions and a proper kernel regression classifier that minimizes the leave-one-out cross-validation [15] on cross-entropy error of the training data given the classifier. The "Vizier" engine searches through a large set of possible classifiers within user specifications, and stops either when all possible choices are exhausted or when a time limit given by the user is reached.

Most physicians prefer using a 2D slice as a query to access digital databases. Though our framework and system design are for 3D volumetric images, 2D slices can be treated as basic image units as well. In this study, we have used three pathology types: blood,infarct and normal brain images; we used 2D slices as basic units. The total 3D image set S_{3D} is randomly divided (within each class) into a training set containing two thirds of S_{3D} (31) and a hold-out test set containing one third of S_{3D} (17), amounting to a total of 1250 2D slices. Care is taken to separate the test set and training set in such a way that there are no 2D slices from the same 3D brain belong to both training and testing sets.

4.4 Hierarchical Classifiers

An image classifier is simply a by-product of the process of feature subset evaluation through classification. The performance of the classifier may predict how well the selected feature subset will behave during image retrieval. For example, we can use a naive Bayes classifier as a 3D image classifier built on top of the 2D image classifiers, using the ratios $r_S = n_S/n$ and $r_B = n_B/n$ as two 3D image features, where n_N, n_S, n_B are the numbers of predicted normal, stroke and blood

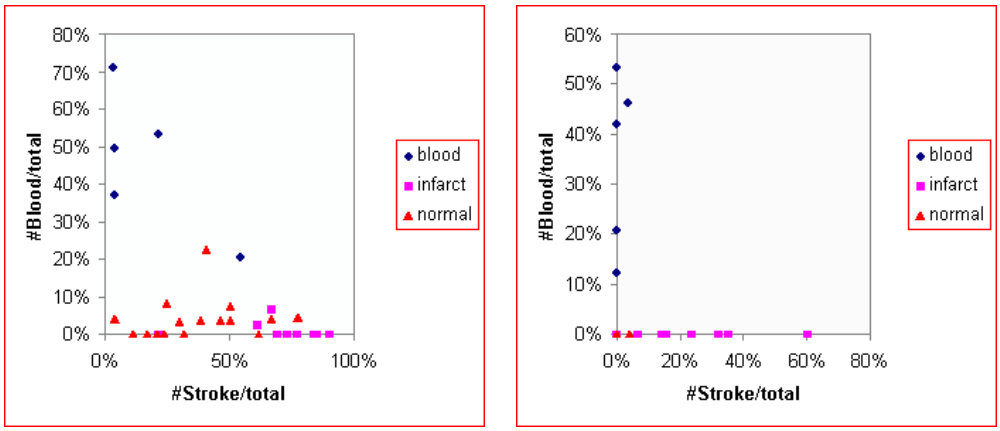

Initial distribution Final distribution

Figure 9: The 3D image points are clustering in the two-ratio feature space while increasing the false negative penalty value of the 2D three-class classifier. The X-axis is r_S and Y-axis is r_B with learned weights 0.5 and 1 respectively.

2D images from the same 3D image, and $n = n_N + n_S + n_B$. The image distribution in this two-dimensional feature space can be observed in Figure 9. From these feature spaces, one can observe that normal and blood cases are better separated than the normal and stroke cases. Using Bayes law, this probability can be expressed as $P(c|[r_S, r_B]) = \frac{P([r_S,r_B]|c)P(c)}{P([r_S,r_B])}$. A *cost matrix* can be imposed to bias the classifier. For example, a *false negative penalty* $w > 1$ is incurred whenever a pathological image is classified as normal, whereas a unit cost or zero cost is incurred when a normal image is classified as pathological or when a chosen class is the correct class, respectively. The performance of such a 3D image classifier (when $w = 4$) is shown in the left of Figure 10.

4.5 Image Retrieval and Evaluation

Our approach is ideally suited to tuning an image similarity metric to the specific type of query that a user may submit to the system. As an example, one may simply want to know whether the query image is normal. In this case, the feature subset that is selected and optimally weighted for discriminating three different pathology types may not be optimal for a binary normal/abnormal discrimination. Thus we need to find an alternative feature subset. When we tried this, the locally optimal classifier found a different metric than the one from the ternary classification case. In both cases, Vizier finds a most discriminating feature subset

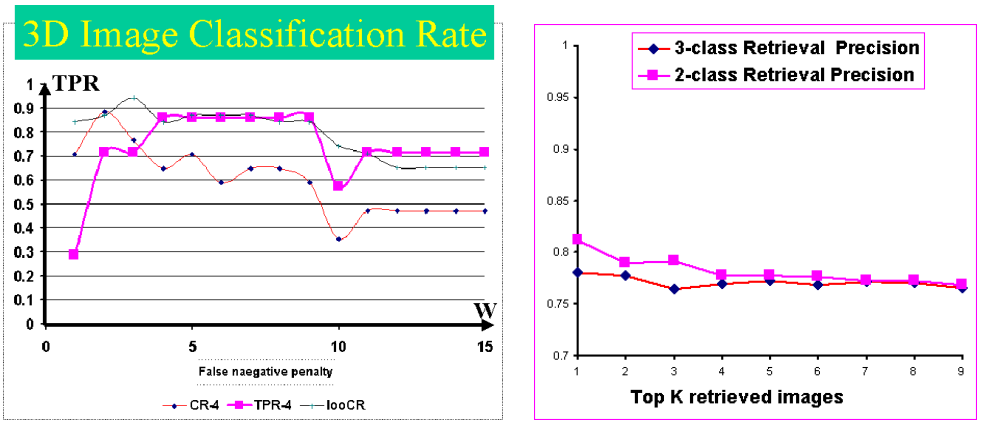

Figure 10: Left (image classification, Bayes classifier): performance of a 3D image classifier on a randomly chosen, held-out test-set when its false negative penalty $w = 4$. TPR-4: true positive rate. CR-4: classification rate. The horizontal axis is the 2D classifier false negative penalty value w. Right (image retrieval, kNN classifier): the mean value of retrieval precision as a function of the top K retrieved images. 2-class: normal, pathology. 3-class: normal, infarct, blood.

containing 9-5 image features — a reduction in indexing feature dimension by nearly 5 to 10 fold. The similarity metric found in image classification can now serve as an image indexing vector for retrieving images in the reduced feature space. The right side of Figure 10 shows the mean retrieval precision rate for the held-out test images, one for the three-class case (normal, blood, infarct) and one for the two-class (normal, abnormal) case. One can observe a slightly better performance for the 2-class than for the 3-class image set. This is to be expected since 2-class classification leaves less space for errors to be made than 3-class classification. However, in this problem the difficult class separation is between normals and strokes, which can be observed from the original image feature values and 2D classifier output (Figure 9), thus the improvement in 2-class is minimal.

Given near 80% precision rate on average for image retrieval, this result implies that in average 8 out of 10 top-ranked retrieved images have the same pathology as the query image. Figure 11 shows two retrieval results for pathology cases: top – blood, bottom – infarct.

5 Discussion and Conclusion

Under our classification-driven semantic-based image retrieval framework, image classification is used as a tool for off-line feature space reduction. We have shown

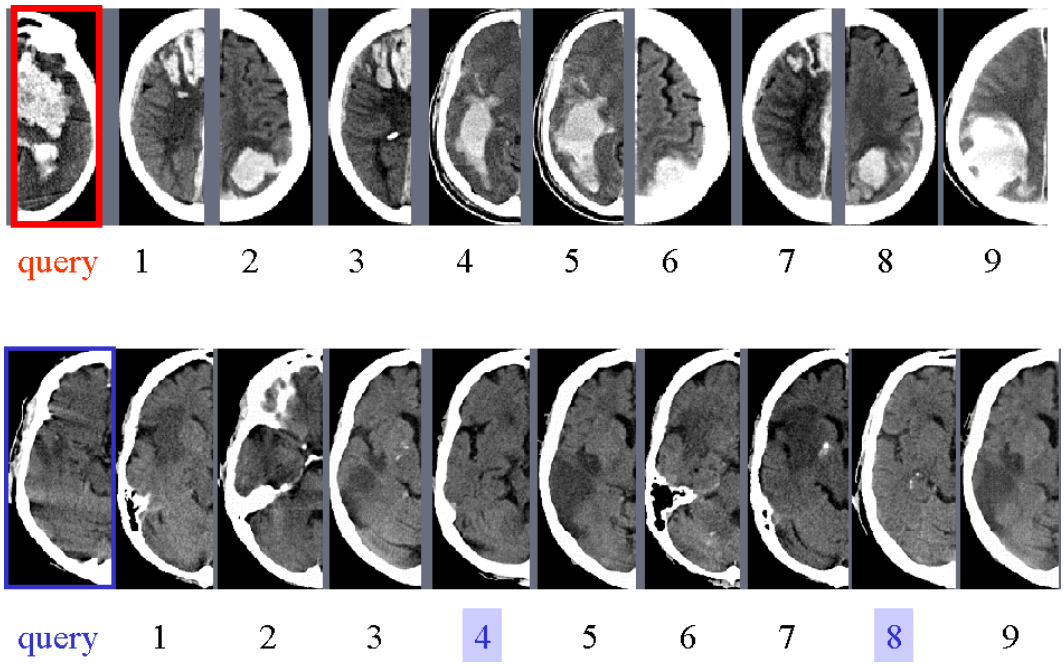

Figure 11: Top left most: query image with acute blood, bottom left most: query image with bland infarct. The first nine retrieved half slices follow, from left to right in descending order of similarity. The pathologies on the top row retrieved images are all acute blood. The pathologies on the bottom row retrieved images are: infarct, infarct, infarct, normal, infarct, infarct, infarct, normal, infarct.

in Table 3 that an initial feature space with 46 dimensions can be reduced to 2-15 dimensions (3-24 fold) with increased discriminating power (better classification rates). It is interesting to notice that the best classification rate improvement is usually associated with the least feature dimension reduction rate and vice versa. This seems to suggest a tradeoff between feature space dimensionality and classification rates. Further study on this topic can be found in [27].

Our effort in looking for the best automated methods for feature space reduction avoids determining image indexing features subjectively. Though it is done off-line, given the stability of image classes in medical images, an on-line user feedback guided learning can still be carried out to fine tuning to each user's specific need.

The selected feature dimensions form the basis for on-line image indexing at retrieval time and provide us a better understanding of the problem at hand. We continue this line of research on discriminative image feature subspace reduction in various applications and algorithm development [12, 28, 27]. Our method provides the generality and potential to scale up to much larger and different biomedical image databases. Figure 12 demonstrates a JAVA image interface for our adaptive classification-driven neuroimage retrieval system.

In this work, we have only used one type of image features extracted from pathology neuroimages, that is a statistical characterization of brain asymmetry. Initial image features are definitely not limited to brain asymmetry alone. Currently, we are exploring various types of image features for neuroimage and other biomedical image databases with an initial dimension exceeding 10,000 [12, 28]. Care should be taken on how to systematically reduce the dimension for discriminative subspace induction without overfitting.

As pointed out in [4]: "To date, all too often image analysis algorithm development ignores the analysis of different abnormal, pathological or disease states". For example, work on neuroimage analysis has been concentrated more on morphological variations of normal brains [3, 6] or brains with mental disorders [22] using high resolution, high density MRI data. Indeed, pathological images present many computational challenges in registration and segmentation. Lacking available robust registration algorithms for pathological volumetric neuroimage registration, we have chosen to find the ideal midsagittal plane in all neuroimages first to align the 3D brain images up to a pitch angle. The exploration of statistical brain asymmetry features provides further understanding of alternative image features other than commonly used color or texture features. We consider our effort a small step in the direction of automatic pathological image analysis, indexing and retrieval.

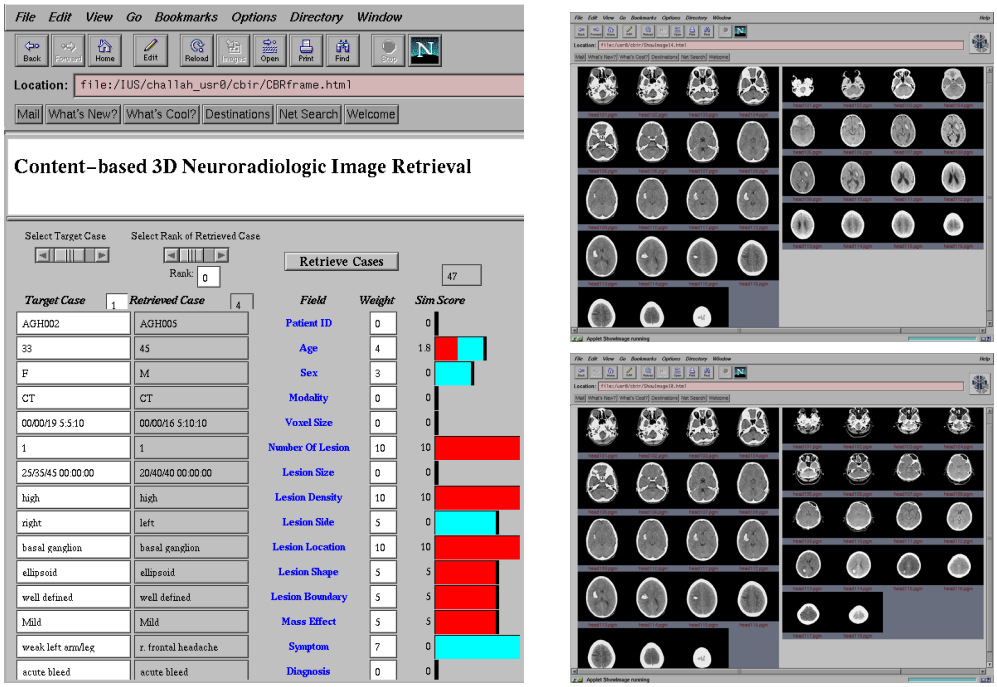

Figure 12: Top: a JAVA user interface of our semantic-based 3D Neuroimage Retrieval System, under development by Dr. Liu et al at the Robotics Institute of Carnegie Mellon University. Two right panels: the netscape screens show one query image on the left with *right basal ganglion acute blood* (shown as a set of 2D slices), the most similar image on the right (top right panel)) and the second most similar image (bottom right panel) retrieved from an image database of more than 100 pathological, volumetric neuroimages.

Retrieving images by semantic content is a new kind of medical database accessing capability, which will provide a practical means for applications in clinical practice and medical education, including on-line consultation, differential diagnosis, surgical planning, recovery/outcome evaluation, and tele-medicine.

Acknowledgments

The authors would like to thank M. Buzoianu for carrying out experiments on discriminant analysis as a summer project. This research is supported in part by the Allegheny-Singer Research Institute under prime contract through the Advanced Technology Program of the National Institute of Standards and Technol-

ogy (NIST#70NANB5H1183) and in part by NIH National Cancer Institute Unconventional Innovation Program, award # = N01-CO-07119.

References

[1] W.W. Chu, F.C. Alfonso, and K.T. Ricky. Knowledge-based image retrieval with spatial and temporal constructs. *IEEE Transactions on Knowledge and Data Engineering*, 10(6):872–888, 1998.

[2] I.J. Cox, L. Miller, T.P. Minka, T.V. Papathomas, and P.N. Yianilos. The bayesian image retrieval system, PicHunter: theory, implementation, and psychophisical. *IEEE transactions on image processing*, 9(1):20–37, 2000.

[3] C. Davatzikos, M. Vaillant, S. Resnick, J.L. Prince, S. Letovsky, and R.N. Bryan. A computerized approach for morphological analysis of the corpus callosum. *Comp. Ass. Tomography.*, 20:88–97, Jan./Feb. 1996.

[4] J.S. Duncan and N. Ayache. Medical image analysis: Progress over two decades and the challenges ahead. *IEEE Transactions on Pattern Analysis and Machine Intelligence*, 22(1):85,106, 2000.

[5] D. Faloutsos, R. Barber, M. Flickner, J. Hafner, W. Niblack, D. Petkovic, and W. Equitz. Efficient and effective querying by image content. *Journal of Intelligent Information Systems*, 1994.

[6] R. Guillemaud, M. Sakuma, P. Marais, J. Feldmar, R. Crow, L. DeLisi, A. Zisserman, and M. Brady. Cerebral symmetry analysis from mri scans. *Psychiatry Research Neuroimaging*, 1998.

[7] D. L. G. Hill, P.G. Batchelor, M. Holden, and D. J. Hawkes. Medical image registration. *Physics in Medicine and Biology*, 46:1–45, 2001.

[8] H.K. Huang and R.K. Taira. Infrastructure design of a picture archiving and communication system. *American Journal of Roentgenology*, 158:743–749, 1992.

[9] Y. Liu, R.T. Collins, and W.E. Rothfus. Robust Midsagittal Plane Extraction from Normal and Pathological 3D Neuroradiology Images. *IEEE Transactions on Medical Imaging*, 20(3), March 2001.

[10] Y. Liu and F. Dellaert. A Classification-based Similarity Metric for 3D Image Retrieval. In *Proceedings of Computer Vision and Pattern Recognition Conference (CVPR'98)*, pages 800–805, Santa Barbara, June 1998. IEEE Computer Society Press.

[11] Y. Liu, F. Dellaert, W.E. Rothfus, A. Moore, J. Schneider, and T. Kanade. Classification-driven pathological neuroimage retrieval using statistical asymmetry measures. In *International Conference on Medical Imaging Computing and Comptuer Assisted Intervention (MICCAI 2001)*. Springer, October 2001.

[12] Y. Liu, T. Zhao, and J. Zhang. Learning discriminant features in multispectrual biological images. In *2002 IEEE International Symposium on Biomedical Imaging: Macro to Nano*, July 2002.

[13] F. Maes, A. Collignon, D. Vandermeulun, G. Marchal, and P. Suetens. Multimodality image registration by maximization of mutual information. *IEEE Transactions on Medical Imaging*, 16(2):187,198, 1997.

[14] T.P. Minka and R. W. Picard. Interactive learning with a "societry of models". *Pattern Recognition*, 30(4):565–581, 1995.

[15] A. W. Moore, D. J. Hill, and M. P. Johnson. An Empirical Investigation of Brute Force to choose Features, Smoothers and Function Approximators. In S. Hanson, S. Judd, and T. Petsche, editors, *Computational Learning Theory and Natural Learning Systems, Volume 3*. MIT Press, 1994.

[16] Virage Inc. Home page. http://www.virage.com.

[17] A. Pentland, R.W. Picard, and S. Sclaroff. Photobook: Content-based manipulation of image databases. *IJCV*, 18(3):233–254, June 1996.

[18] Y. Rubner, C. Tomasi, and L. Guibas. A metric for distributions with applications to image databases. In *Proceeding of Sixth International Conference on Computer Vision*, pages 59,66. Narosa, 1998.

[19] J. Schneider and A.W. Moore. A locally weighted learning tutorial using vizier 1.0. *tech. report CMU-RI-TR-00-18, Robotics Institute, Carnegie Mellon*, 1997.

[20] H.D. Tagare, C.C. Jaffe, and J. Duncan. Medical image databases: a content-based retrieval approach. *J Am Med Inform Assoc*, 4(3):184–198, May 1997.

[21] J. Talairach and P. Tournoux. *Co-Planar Steriotaxic Atlas of the Human Brain*. Thieme Medical Publishers, 1988.

[22] P.M. Thompson, C. Schwartz, and A.W. Toga. High-resolution random mesh algorithms for creating a probabilistic 3d surface atlas of the human brain. *Neuroimage*, 3(1):19–34, Feb 1996.

[23] W.N. Venables and B.D. Ripley. *Modern Applied Statistics with Splus, 2nd edition*. Springer-Verlag, London, Paris, Tokyo, 1997.

[24] James Z. Wang, Jia Li, and Wiederhold Gio. Simplicity: Semantics-sensitive integrated matching for picture libraries. *IEEE Transactions on Pattern Analysis and Machine Intelligence*, 23(9), Septermber 2001.

[25] J. West, M. Fitzpatrick, and et al. Comparison and evaluation of retrospective intermodality brain image registration techniques. *Journal of Computer Assisted Tomography*, 21:554–566, July/August 1997.

[26] S.T. Wong and H.K. Huang. Design methods and architectural issues of integrated medical image data base systems. *Comput Med Imaging Graph*, 20(4):285–299, July 1996.

[27] J. Zhang and Y. Liu. SVM decision boundary based discriminative subspace induction. Technical Report CMU-RI-TR-02-15, The Robotics Institute, Carnegie Mellon University, Pittsburgh, PA, 2002.

[28] J. Zhang, Y. Liu, and T. Zhao. SVM based feature screening applied to hierarchical cervial cancer detection. In *Proceeding of International Conference on Diagnostic Imaging and Analysis (ICDIA 2002)*, Shanghai, China, August 2002.